

Supporting Information to

**Impact of Anchoring Groups on Ballistic Transport:  
Single Molecule vs. Monolayer Junctions**

Veronika Obersteiner<sup>†</sup>, David A. Egger <sup>†, ‡</sup>, and Egbert Zojer <sup>†</sup>

<sup>†</sup> *Institute of Solid State Physics, NAWI Graz, Graz University of Technology, Petersgasse 16,  
8010 Graz, Austria*

<sup>‡</sup> *Department of Materials and Interfaces, Weizmann Institute of Science, Rehovoth 76100,  
Israel*

## Additional Data

### 1. Variation of the molecular packing density

The density of the molecules bridging the electrodes was varied by increasing the size of the unit cell and consecutively removing molecules. Figure S1 a-e shows the different unit cells for molecular packing densities of  $\Theta=1$ ,  $1/2$ ,  $1/4$ ,  $1/8$  and  $1/16$ , respectively. For example, the 50% packing density,  $\Theta=1/2$ , was achieved by doubling the  $(2 \times 2)$  surface unit cell in  $x$ -direction and deleting one molecule. The gold atoms situated laterally in-between the remaining molecule were set to their bulk atomic positions (eliminating surface reconstructions due to thiolate-Au bonds in regions, where molecules have been removed). Lower packing densities were generated by alternately doubling the unit cells in  $y$ - and  $x$ -direction, in all cases retaining only one molecule per unit cell. For all packing densities, the molecules are kept in the equilibrium geometry found for  $\Theta=1$ .

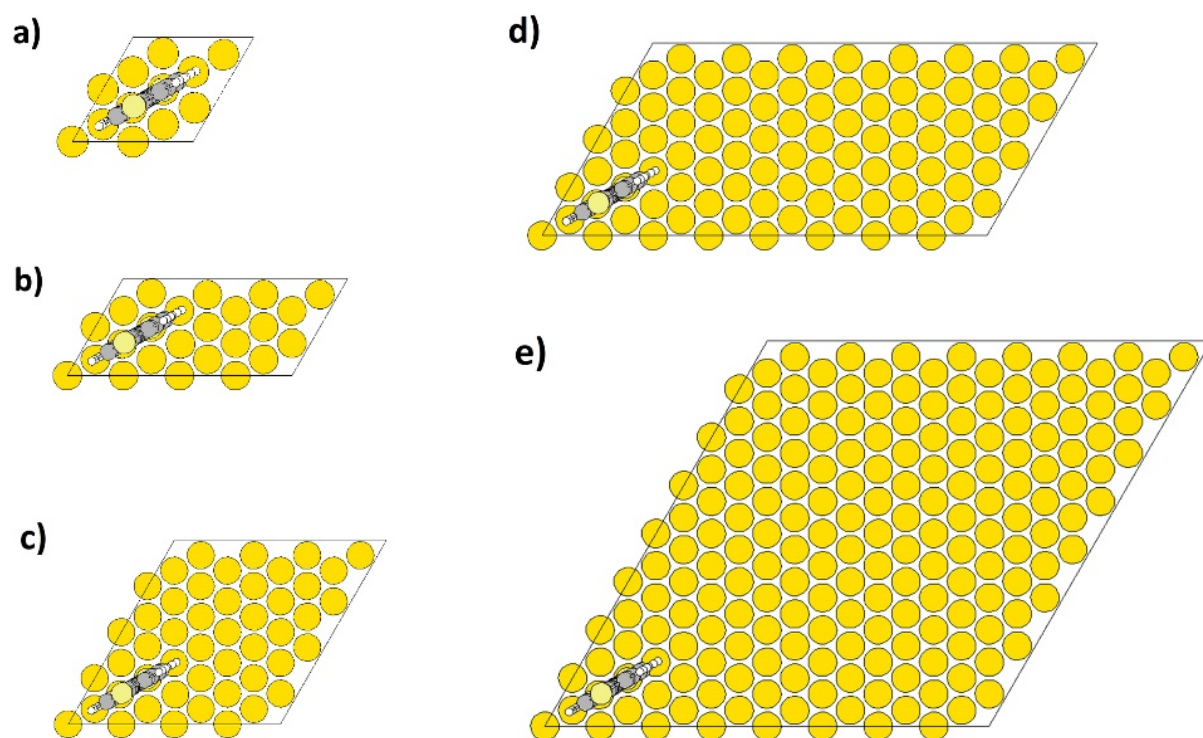


**Figure S1:** Top view of molecular junctions without their top electrodes at different molecular packing densities of (a)  $\Theta=1$ , (b)  $\Theta=1/2$ , (c)  $\Theta=1/4$ , (d)  $\Theta=1/8$ , and (e)  $\Theta=1/16$ .

## 2. Current-Voltage Characteristics

Figure S2 shows the current-voltage characteristics of the investigated systems for the single molecule junction in a voltage range between 0 V and 0.50 V. At 0.2 V we can identify a sequence of currents following:  $S \approx NC > Pyr_{ad} > CH_2S > Pyr$ . This sequence is the same as for the zero-bias conductance  $G(E_F) = T(E_F) \cdot G_0$  shown in Figure 2 of the main text. The values for  $G(E_F)$  are summarized in Table S1.

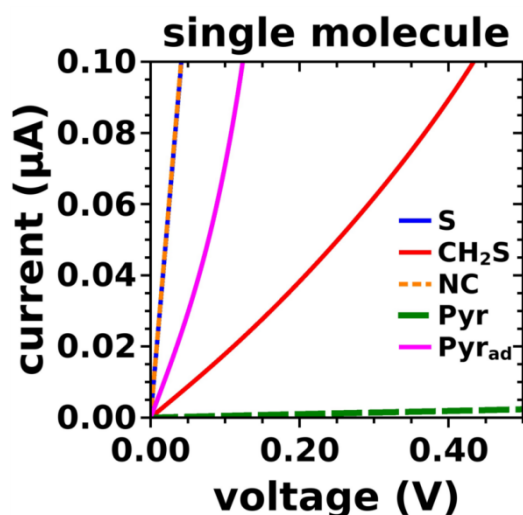


**Figure S2:** : Calculated current-voltage characteristics of the (-S), (-CH<sub>2</sub>S), (-NC), (-Pyr) and (-Pyr<sub>ad</sub>) systems for the model of a single molecule junction with a packing density  $\Theta=1/16$ . This figure is a zoom of Figures 2a) of the main manuscript.

**Table S1:** Zero-bias conductance  $G(E_F) = T(E_F) \cdot G_0$  for full monolayer junctions,  $\Theta=1$  and single molecule junctions,  $\Theta=1/16$ .  $G_0$  here refers to the quantum of conductance that corresponds to  $2e^2/h$ .

	$G(E_F) [G_0]$ at $\Theta=1$	$G(E_F) [G_0]$ at $\Theta=1/16$
(-S)	0.014	0.030
(-CH <sub>2</sub> S)	0.001	0.002
(-NC)	0.057	0.032
(-Pyr)	0.059	6e-05
(-Pyr <sub>ad</sub> )	0.133	0.004

Figure S3 shows the voltage dependent current per molecule for the investigated systems at different molecular packing densities  $\Theta$ , ranging from full monolayer,  $\Theta=1$ , to  $\Theta=1/2$ ,  $\Theta=1/4$ ,  $\Theta=1/8$  and finally the single molecule situation,  $\Theta=1/16$ .

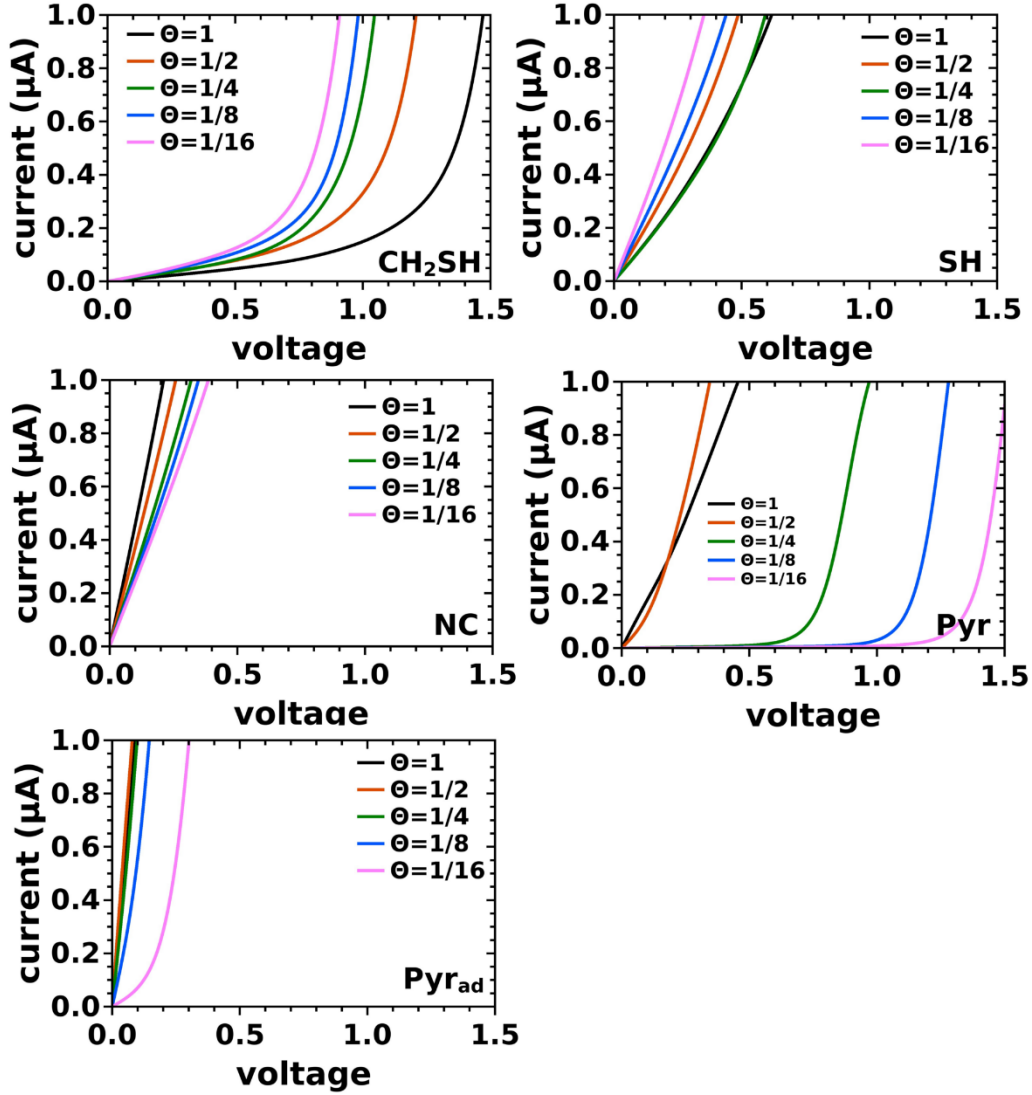


**Figure S3:** Voltage dependent current per molecule for ( $-\text{CH}_2\text{SH}$ ), ( $-\text{SH}$ ), ( $-\text{NC}$ ), ( $-\text{Pyr}$ ) and ( $-\text{Pyr}_{\text{ad}}$ ) junctions at different molecular packing densities  $\Theta$  derived from the transmission functions via the Landauer equation.

### 3. Cumulative charge transfer

Further insight into the implications of the charge rearrangements can be obtained by integrating  $\Delta\rho$  over the transport direction,  $z$ :  $Q(z) = \int_0^z \Delta\rho(z') dz'$ . This yields the total amount of transferred charge per unit cell from left to right of a plane at  $z$ . Figure S4 shows the cumulative charge transfer of the investigated systems at the highest and lowest considered packing densities. Dashed grey lines indicate the positions of the innermost gold layers. Note that whenever  $Q(z)$  reaches zero that means that no net charge is transferred across the plane at  $z$ . The triangular shapes of  $Q(z)$  in the molecular regions at  $\Theta=1/16$  with the zero-crossing in the middle of the junction are indicative of a polarization of the molecular backbones arising from the molecule-metal interaction. The wiggles at  $\Theta=1$  for ( $-\text{Pyr}$ ) and ( $-\text{Pyr}_{\text{ad}}$ ) are indicative of a polarization of the molecular backbones arising from the molecule-metal interaction.

$\text{Pyr}_{\text{ad}}$ ) along the molecular backbones indicate short-range polarization effects due to Fermi-level pinning.

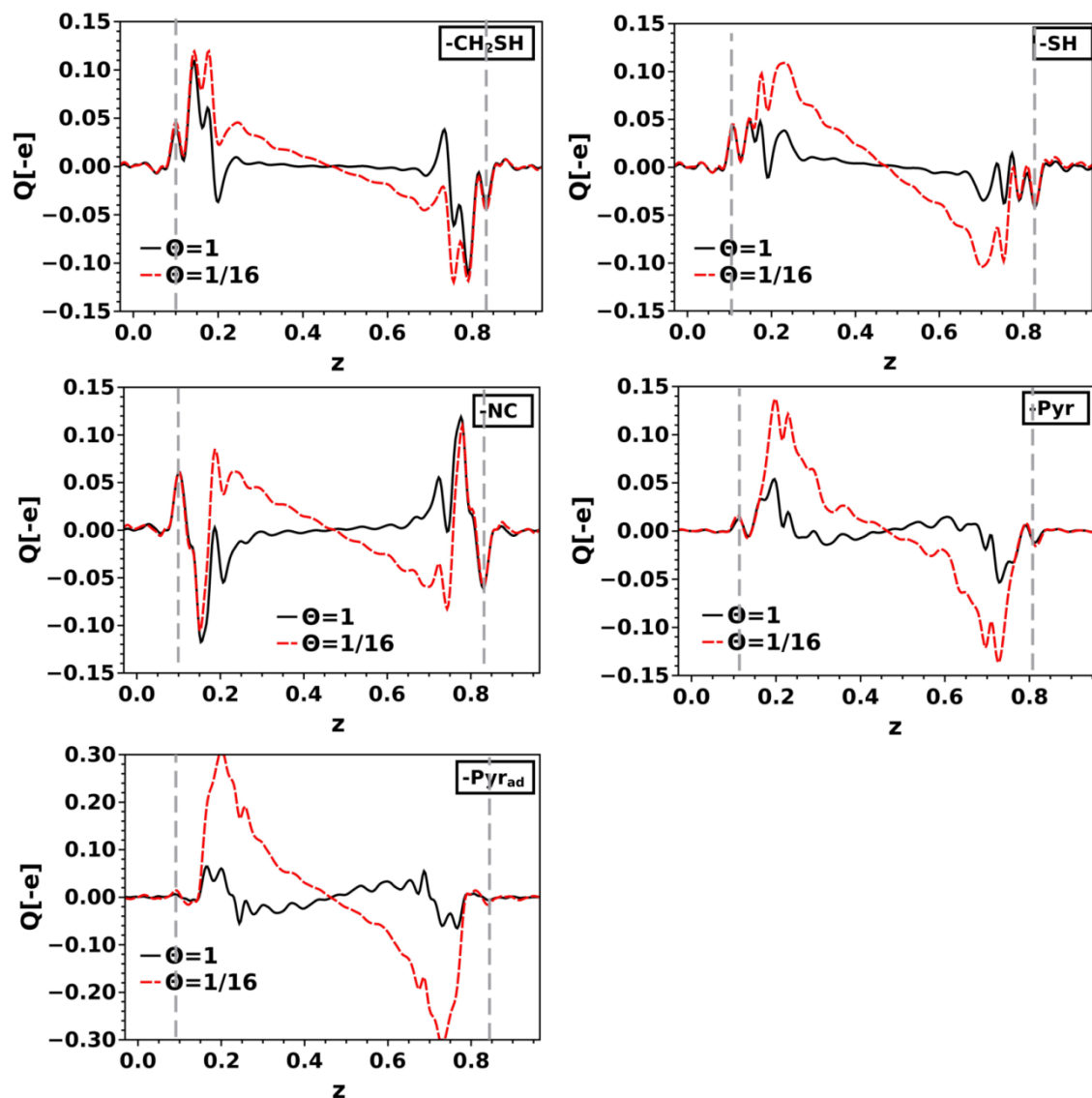


**Figure S4:** Cumulative charge transfer  $Q$  for all investigated molecular junctions with different docking groups: ( $-\text{CH}_2\text{S}$ ), ( $-\text{S}$ ), ( $-\text{NC}$ ), ( $-\text{Pyr}$ ) and ( $-\text{Pyr}_{\text{ad}}$ ) at different packing densities  $\Theta$ .

#### 4. Evolution of the Bond Dipole with Packing Density

Figure S5 shows the ( $x$ - $y$ )-plane averaged change in the electrostatic energy due to metal-molecule bonding of all investigated systems at different molecular packing densities  $\Theta$ . The corresponding contour plots in the plane of the molecules can be found in the main text in Figure 5. The values for  $\Delta E_{\text{BD}}$  in Table 1 of the main text are obtained from these plane-averaged quantities as the value in the center of the molecular junction.

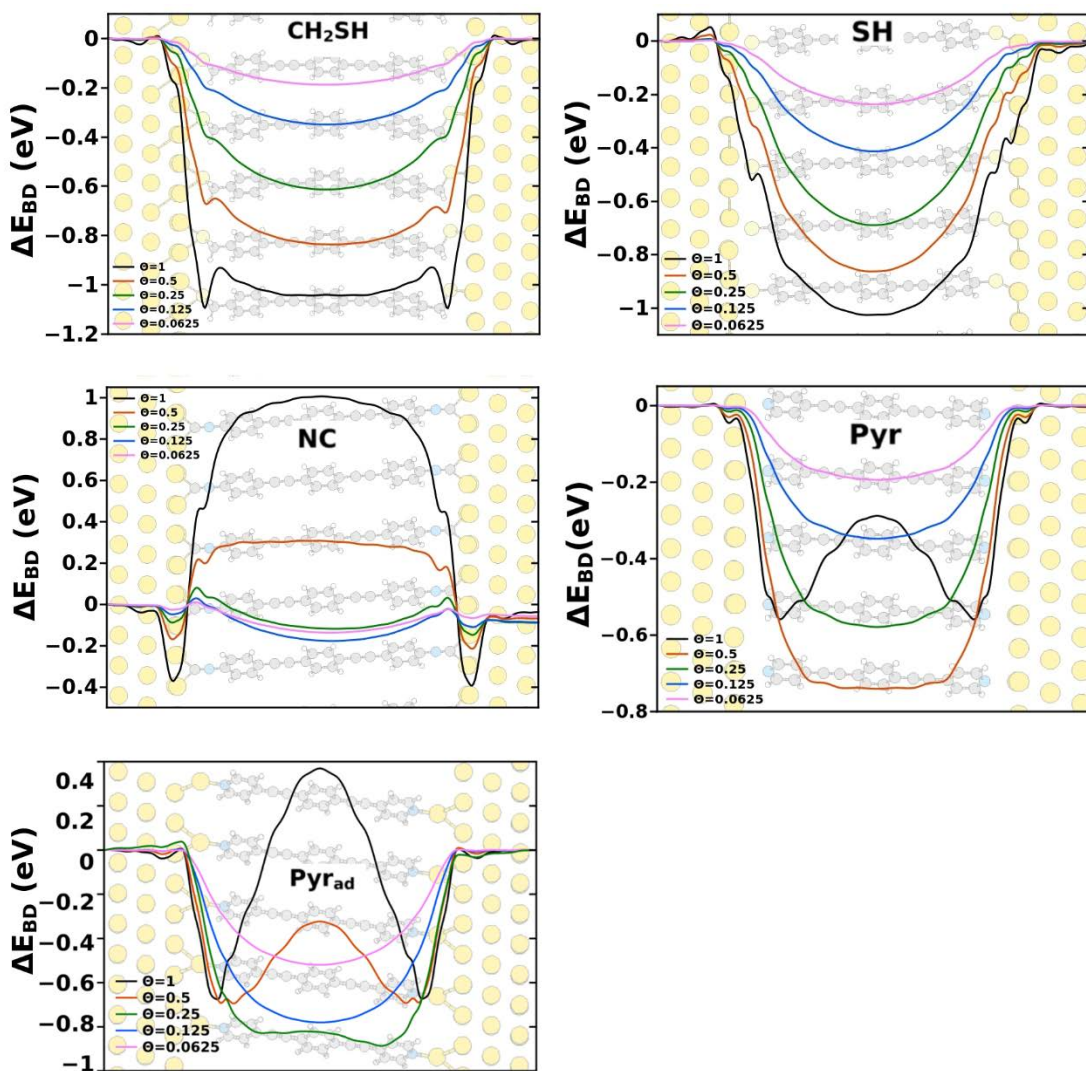


**Figure S5:** Bond dipole  $\Delta E_{BD}$  for all investigated molecular junctions with different docking groups:  $(-CH_2S)$ ,  $(-S)$ ,  $(-NC)$ ,  $(-Pyr)$  and  $(-Pyr_{ad})$  at different packing densities  $\Theta$ .

## 5. Molecular Properties of investigated systems

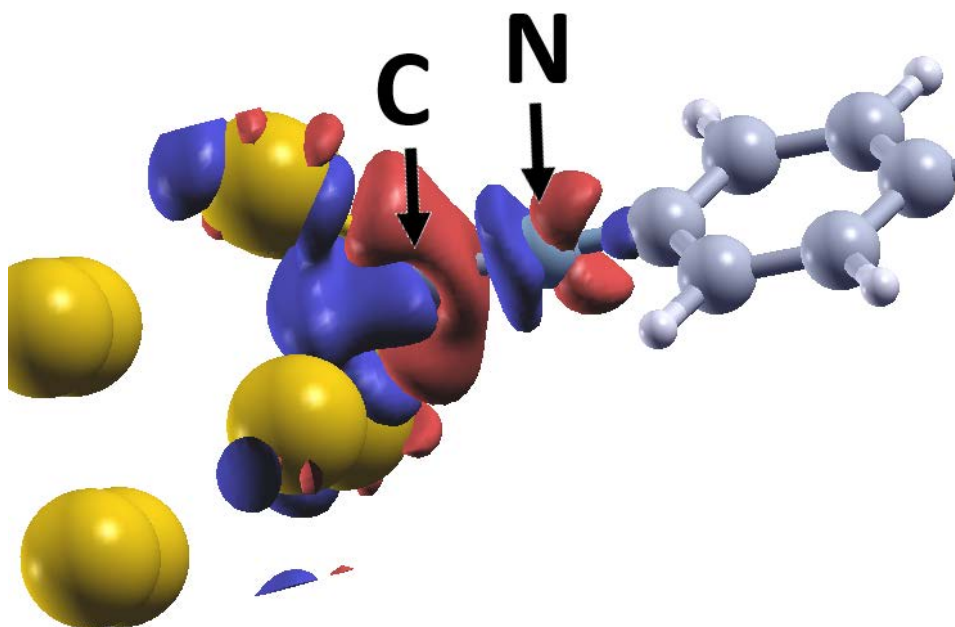
**Table S2:** Energies of the frontier  $\pi$ -orbitals of the isolated molecules,  $\epsilon_{HOMO}$  and  $\epsilon_{LUMO}$ , relative to the vacuum level realigned considering the work function of the electrodes (details see main manuscript), obtained from VASP calculations for the lowest molecular packing density at  $\Theta=1/16$  for  $(-CH_2S)$ ,  $(-S)$ ,  $(-NC)$ ,  $(-Pyr)$  and  $(-Pyr_{ad})$  systems.

	-S	-CH <sub>2</sub> S	-NC	-Pyr	-Pyr <sub>ad</sub>
$\epsilon_{HOMO}$ [eV]	-4.94	-5.18	-5.73	-5.86	-5.77
$\epsilon_{LUMO}$ [eV]	-2.77	-2.88	-3.61	-3.49	-3.52

	-S	-CH <sub>2</sub> S	-NC	-Pyr	-Pyr <sub>ad</sub>
$\bar{\epsilon}_{\text{HOMO}}$ [eV]	0.24	0.00	-0.55	-0.68	-1.06
$\bar{\epsilon}_{\text{LUMO}}$ [eV]	2.41	2.30	1.57	1.69	1.19

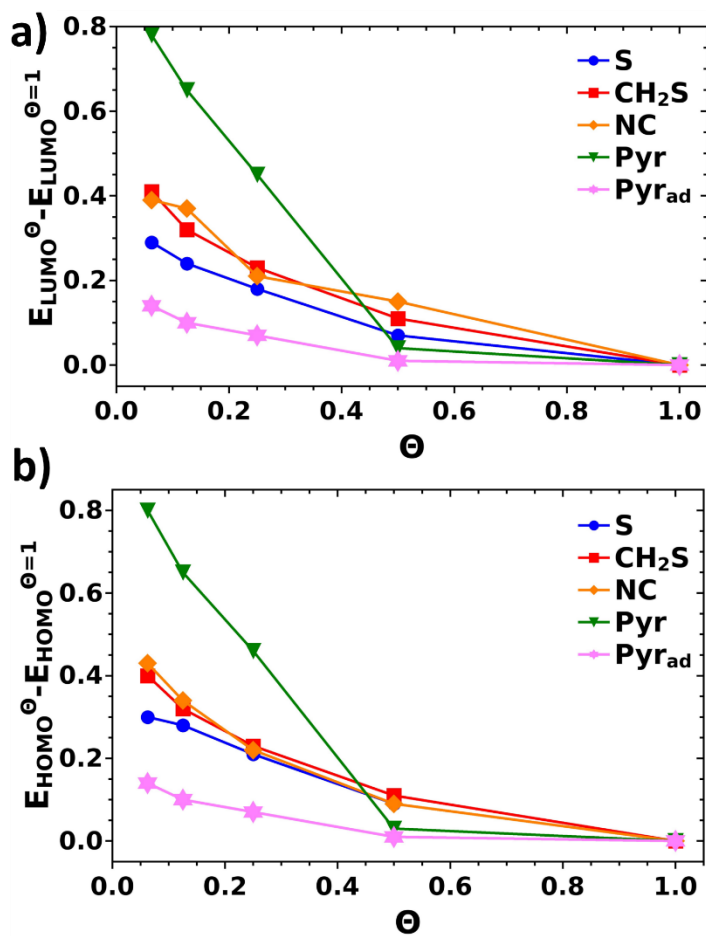
## 6. Bond Formation between (-NC) anchoring group and Au substrate

Figure S6 shows the 3D isodensity representation of the charge rearrangements of the isocyanide linked system at highest packing density. Blue/red regions show electron depletion/accumulation. Black arrows indicate the position of the N and C atom. These charge rearrangements at the interface can be associated with the bond-formation between the -NC group and Au, where electrons are redistributed from the C lone pair to the region between the C atom and the two closest Gold atoms (red regions between the Carbene and the Au-surface). At the same time, the strong electron depletion at the Nitrogen atom (blue lobe between the nitrogen and the carbene) is indicative of a partial transformation from a (N-C) triple to a double bond. This interpretation is supported by the observation that the N-C bond elongates upon adsorption (1.18 Å in the gas phase molecule and 1.22 Å after bonding).



**Figure S6:** 3D isodensity representation of the charge rearrangements of the metal-molecule interface of the (-NC) system at highest packing density. Blue means charge depletion, red means charge accumulation.

## 7. Packing Dependent Peak Positions of HOMO- and LUMO-Derived Bands for all Investigated Systems



**Figure S7:** Packing dependent peak positions of (a) HOMO- and (b) LUMO-derived bands (obtained from PDOS) for all investigated systems, aligned with respect to the energies for full packing density  $\Theta=1$ .



## 8. Packing Dependent Transmission Function for all Investigated Anchoring Groups

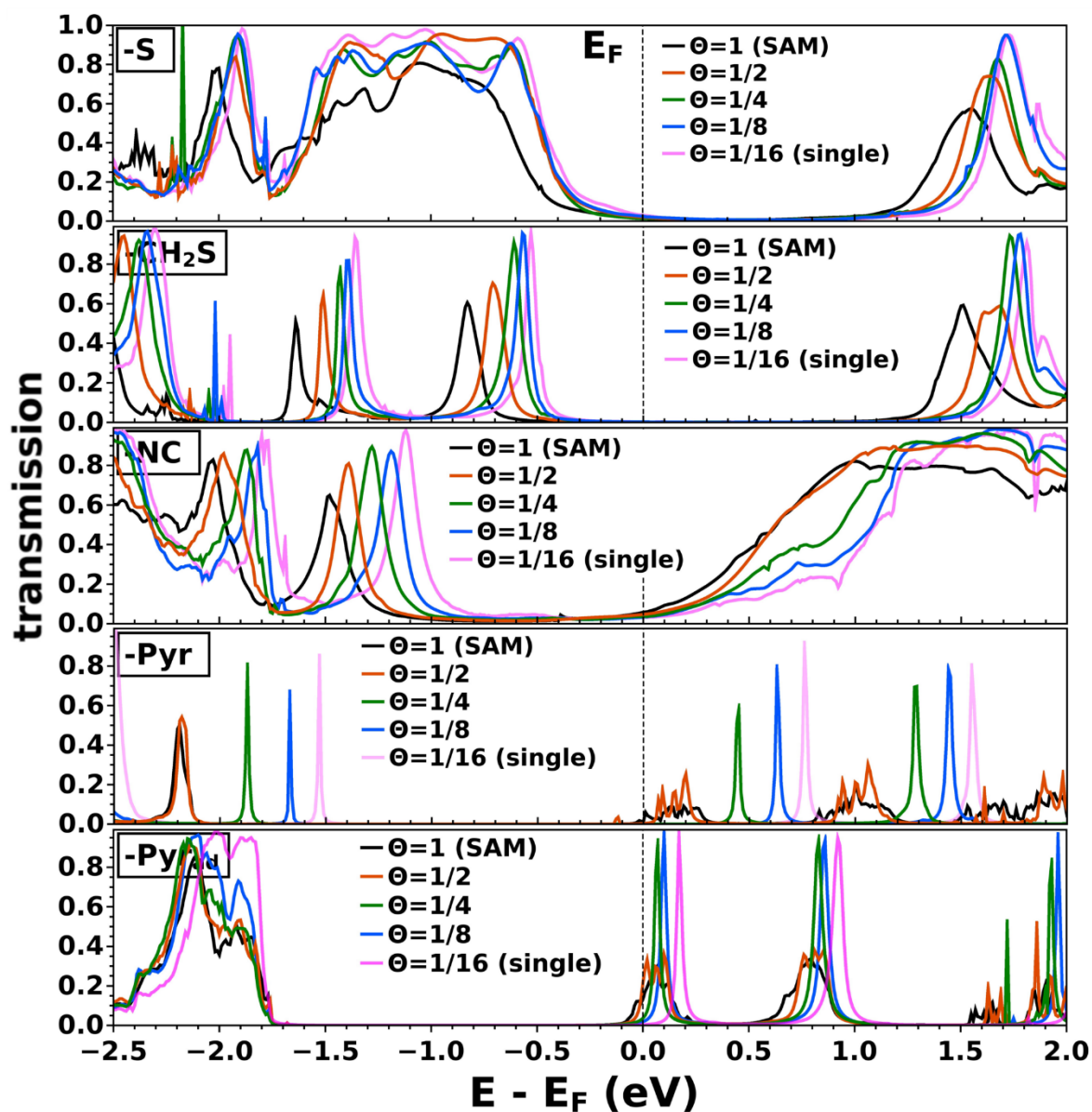


*Figure S8: Calculated (zero-bias) transmission functions of the (-S), (-CH<sub>2</sub>S), (-NC), (-Pyr) and (-Pyr<sub>ad</sub>) systems at different packing densities  $\Theta$ . The Fermi level  $E_F$  is used as the energy reference.*